

Parallel Volume Rendering Algorithms for Computational Flow Imaging

Yingchuan Wu, Jialing Le

China Aerodynamics Research & Development Center

Anzhi He

Applied Physics Department of Nanjing University of Science & Technology of China

Abstract: Computational flow imaging (CFI) uses theoretical predictions of the interaction and transmission of optical waves through theoretical flowfield to generate digital pictures that simulate real observations, but visualizing three-dimensional unstructured data from aerodynamics calculations is challenging because the associated meshes are typically large in size and irregular in both shape and resolution. The goal of this research is to develop a fast, efficient parallel volume rendering algorithm of computational flow imaging (corresponding to shadowgraph, schlieren and interferometric) for parallel distributed-memory supercomputers consisting of a large number of powerful processors. We use a preprocessing procedure that the whole flow field is divided into new regular regions in which the voxels are distributed by x and y coordinates so that the ray-casting and field reconstructing can provide maximum flexibility in the data distribution and rendering steps.

Keywords: Parallel Volume rendering, Computational Flow Imaging

1. Introduction

Computational flow imaging (CFI) is a new approach to flow visualization. It uses theoretical predictions of the interaction and transmission of optical waves through theoretical flowfield to generate digital pictures that simulate real observations. CFI is used to construct flow visualization corresponding to shadowgraph, schlieren, interferometric and Planar Laser Induced Fluorescence (PLIF) images. CFI provides a better insight into the flow physics and CFD code behavior. It is proving to be extremely useful to experimentally validate CFD codes. In essence it is the art and science of generating digital images of theoretical fluid dynamic phenomena in formats that mimic optical observations of real flowfield. Models for the flow measurement processes must therefore be superimposed on the models used to predict the flow behavior.

There are two main challenges in CFI. First, the image recorded is integrated across the three-dimensional flowfield for all CFI numerical processes (except Planar Laser Induced Fluorescence in a thin sheet passed into the flow). Second, the CFD calculation is becoming more complicated in both size and shape, so parallel rendering algorithms of CFI for large dataset should also be developed correspondently.

Report Documentation Page

Report Date 23 Aug 2002	Report Type N/A	Dates Covered (from... to) -
Title and Subtitle Parallel Volume Rendering Algorithms for Computational Flow Imaging	Contract Number	
	Grant Number	
	Program Element Number	
Author(s)	Project Number	
	Task Number	
	Work Unit Number	
Performing Organization Name(s) and Address(es) Institute of Theoretical and Applied Mechanics Institutskaya 4/1 Novosibirsk 530090 Russia	Performing Organization Report Number	
	Sponsor/Monitor's Acronym(s)	
Sponsoring/Monitoring Agency Name(s) and Address(es) EOARD PSC 802 Box 14 FPO 09499-0014	Sponsor/Monitor's Report Number(s)	
Distribution/Availability Statement Approved for public release, distribution unlimited		
Supplementary Notes See also ADM001433, Conference held International Conference on Methods of Aerophysical Research (11th) Held in Novosibirsk, Russia on 1-7 Jul 2002		
Abstract		
Subject Terms		
Report Classification unclassified	Classification of this page unclassified	
Classification of Abstract unclassified	Limitation of Abstract UU	
Number of Pages 6		

Some of the former authors^{1,2,3} only involve simple two-dimensional problems. The methods of Tamura⁴, Yates⁵ and Lanen⁶ are actually three-dimensional, however, for the line-of-sight integration scheme, not considering that there are intersecting or overlapping of multi-grids CFD solutions, they would repeat calculating some integral segments along ray path.

We develop a parallel volume rendering method available for Computational Flow Imaging to translate curvilinear multiple overlapping grids CFD resolutions into new rectilinear multi-blocks data fields in order to eliminate errors caused by intersected or overlapped parts of the CFD grids. A preprocessing procedure is used to divided the whole flow field into new regular regions in which the voxels are distributed by x and y coordinates to increase the searching speed. This parallel algorithm is implemented in a linux-based Beowulf parallel computing system.

2. Optical modeling

Shadowgraphs, schlieren and interferometric techniques commonly used to visualize refractive index or density changes in flow fields. Shadowgraph systems are often used where the density gradients are large. This technique also can accommodate large subjects, is relatively simple in terms of materials required and in terms of cost is probably the least expensive technique to set-up and operate. Schlieren systems are intermediate in terms of sensitivity, system complexity and cost. Schlieren systems deserve attention for its relative simplicity (the equipment is straightforward to align), ease of application (little sensitivity to vibrations), low cost (expensive laser sources are not required) and satisfactory accuracy of results. Interferometric techniques are usually highly sensitive, complex in set-up, can provide quantitative information but are expensive systems and can only deal with relatively small subjects.

For three-dimensional flow fields, in order to evaluate line-of-sight integration through a discrete three-dimensional field, an algorithm has been developed which calculates the values of the appropriate integrand at certain points, after which the integration is performed according the trapezoidal rule.

Shadowgraph systems respond to the second derivative of flow density where as schlieren systems respond to the first derivative. If the light path length is divided into n segments, for shadowgraph systems, the distributions for the optical intensities are

$$I \propto \int_{z_1}^{z_2} \left(\frac{\partial^2 \rho}{\partial x^2} + \frac{\partial^2 \rho}{\partial y^2} \right) dz = \sum_{i=1}^n \left(\frac{\partial^2 \rho_i}{\partial x^2} + \frac{\partial^2 \rho_i}{\partial y^2} \right) \Delta z_i \quad (2.1)$$

For schlieren systems, if the knife-edge or color filter is vertical, the optical intensities are

$$I \propto \int_{z_1}^{z_2} \frac{\partial \rho}{\partial x} dz = \sum_{i=1}^n \frac{\partial \rho_i}{\partial x} \Delta z_i \quad (2.2)$$

If the knife-edge or color filter is horizontal, the optical intensities are

$$I \propto \int_{z_1}^{z_2} \frac{\partial \rho}{\partial y} dz = \sum_{i=1}^n \frac{\partial \rho_i}{\partial y} \Delta z_i \quad (2.3)$$

For optical Mach-Zehnder or holographic interferometer, the light intensity I is proportional to fringe shift F by⁷

$$I \sim \cos^2(\pi F), \quad (2.4)$$

In order to calculate the Fringe shift, according to Mach-Zehnder or holographic interferometry, the bright fringes satisfy the equation⁸:

$$2\varepsilon x + \int_{s_i} [n(x, y, z) - n_0] dz = i\lambda \quad (i = 1, 2, 3, \dots) \quad (2.5)$$

where $[n(x, y, z) - n_0]$ is the refractive index relative to some reference field n_0 and the path integral is evaluated along the ray path s_i , ε is the difference of the angle of two glass plates P_1 and P_2 , i is the integer fringe shift, λ is the wavelength of the light source.

When there is no disturb in the flowfield of the test volume, if $\varepsilon = 0$, the beams reaching the photo plane are with the same phase, so there are no reference fringes (infinite-fringe); if $\varepsilon > 0$ or $\varepsilon < 0$, the recombined beams will interfere and produce reference fringes (finite-fringe).

The reference fringes of Eq. (2.1) and the following equations of this section are all vertical. To get horizontal reference fringes, we can use $2\varepsilon y$ instead of term $2\varepsilon x$ of these equations.

Using continuous fringe shift F instead of i as function of $n(x, y, z)$, we have

$$F(x, y) = \frac{2\varepsilon x}{\lambda} + \frac{1}{\lambda} \int_{z_1}^{z_2} [n(x, y, z) - n_0] dz, \quad (2.6)$$

The optical path is along z . The limits of integration, z_1 and z_2 represent the length along the optical path length where the index of refraction is varying.

The relation between gas density ρ and refraction index n is Gladstone-Dale equation

$$n - 1 = K\rho, \quad (2.7)$$

For gases of different species, K is not constant. It is

$$K = \sum_i K_i \frac{\rho_i}{\rho} = \sum_i K_i a_i, \quad (2.8)$$

where a_i is the mass fraction and K_i is the G-D constant of the i^{th} specie.

The Eq. (2.6), Eq. (2.7) and Eq. (2.8) constitute the theoretical model of optical Mach-Zehnder or holographic interferometric systems for flow density measurement, if the light path length is divided into n segments in a discrete three-dimensional field, then the fringe shift F is

$$F(x, y) = \frac{2\varepsilon x}{\lambda} + \frac{K}{\lambda} \rho_0 \int_{\xi_1}^{\xi_2} \left(\frac{\rho}{\rho_0} - 1 \right) dz = \frac{2\varepsilon x}{\lambda} + \frac{K}{\lambda} \rho_0 \sum_{i=1}^n \left(\frac{\rho}{\rho_0} - 1 \right) \Delta z_i, \quad (2.9)$$

3. Parallel Volume Rendering

CFI assumes that the considered domain contain a gas with variable optical properties of shadowgraph, schlieren or interferometric. At the volume rendering the domain is projected on the screen in such a way that analyzed function is transformed to a distribution of intensity of light on view plane. This transformation uses integral function given by the relation Eq. (2.1), Eq. (2.2), Eq. (2.3) and Eq. (2.9).

Usually the calculation grids of CFD solutions are multizone, curvilinear or irregular, while the ray path is approximated by a straight lines perpendicular to the image plane⁵. Volume rendering multizone, curvilinear or irregular grids is a hard operation and there are several different ap-

proaches to this problem.

The simplest but most inefficient way is to resample the irregular grid to a regular grid. In order to achieve the necessary accuracy, a high enough sampling rate has to be used what in most cases will make the resulting regular grid volume too large for storage and rendering purposes, not mentioning the time to perform the resampling.

Yates⁴ used a method similar with cell projection. In cell projection, every pixel on the image plane should be projected otherwise not all the segments in a light path are included in the accumulation of the final results. The contribution of each computational cell to the line integral can be found independently. The disadvantage of cell projection is that for intersected or overlapped grids, the overlapped parts of the segments along the light path will be calculated repeatedly and cause integral errors.

Raytracing is expensive than projection because it need to search in the cells to find the voxels intersected by the light, but it can deal with any complex grids of the CFD flow field. Only raytracing can avoid the integral error in multi-grids curvilinear intersecting or overlapping volumetric datasets. In ray tracing, resampling process costs much more times than integral calculation.

We develop a preprocessing procedure to increase the speed of resampling in raytracing. First, voxelization is used to convert CFD grids from their continuous geometric representation into a set of voxels⁹. Then voxels are distributed into regular regions according to the voxels' location. The regular regions created by equally divide the whole flow field along x and y coordinates. At last the voxels in different regions are distributed into different parts of the parallel distributed-memory supercomputers ready for parallel graphic rendering. After the preprocessing procedure, resampling is fast from two aspects. One is that it can be parallely processed. The other is that each sub-region has fewer voxels for searching.

Our parallel algorithm benefit from the parallel distributed-memory supercomputers for the increasing of the number of CPU and the sum of total memories. Additionally, because every line integral process needs to search through all voxels in a block, when we make more blocks with fewer voxels in each block after region dividing, the total searching speed is improved despite of the cost of the voxels' distributing process. This make the performance increased greatly.

Ideally, data should be distributed in such a way that every processor requires the same amount of storage space and incurs the same computational load. Load imbalances are unavoidable because voxels come in different sizes and shapes. The difference in size can be as large as several orders of magnitude due to the adaptive nature of the mesh. Load imbalances are reduced by making all the regions have approximately the same number of voxels.

3 Test Results

For convenience, we have used two examples for our initial experiments. Each example has a small curvilinear grid dataset containing about 0.5 million hexahedral cells. The first example represents shock wave over two bodies in a channel bend. The surface mesh of the dataset is displayed in Figure 1. The first body is a cylinder-cone with the base diameter of 22mm and height of 16mm, and the second one is the square pillar with base size of 16mm \times 16mm and 12mm height. The second example is for examining the hypersonic dynamics of a ball shape (12mm) in the ballistic range. We plan to conduct further tests using a larger dataset with several million cells.

We implemented our volume renderer in the C++ language using MPI message passing¹⁰ for interprocessor communication. All tests were run on a Beowulf parallel computing system built by ourselves. The Beowulf parallel computing system is a distributed-memory architecture which employs a switch-based processor interconnect. Our Beowulf parallel computing system runs on Redhat linux 5.0 and it is populated with 9 nodes based on 800 MHz Pentium III processor and incorporate a 100 Mb/s ethernet switch.

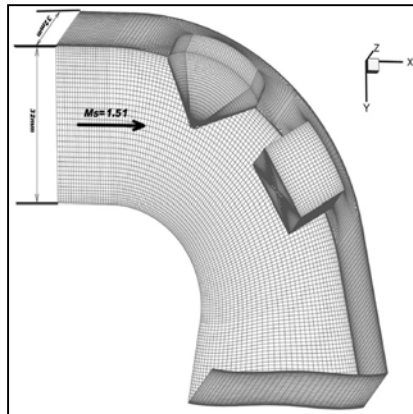


Figure 1 Schematic for shock wave over two bodies in channel bend

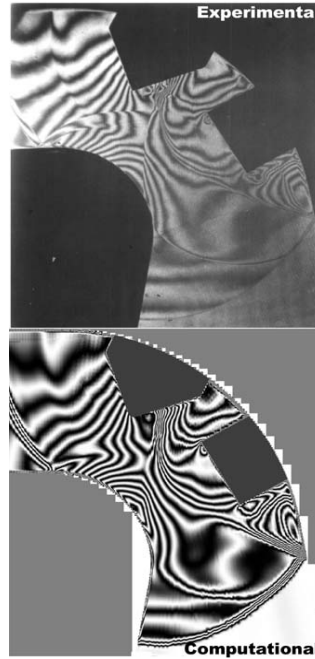


Figure 2 Comparison of experimental and computational interferograms

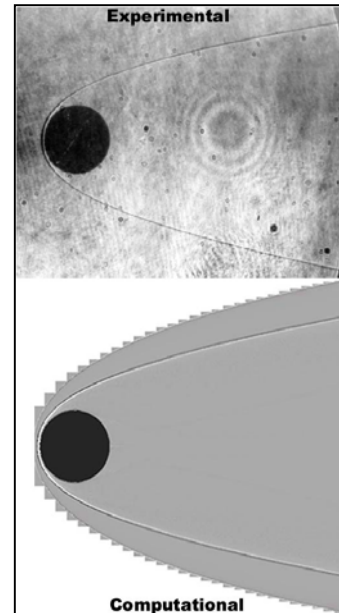


Figure 3 Comparison of experimental and computational shadowgraphs

Figure 2 is a comparison of experimental and computational interferograms of the first example. The test is performed at Mach number M_∞ of 1.51 and wall temperature T_w of 285K. CFD use laminar conservative full N-S equation with TVD scheme in convective terms and with center difference in viscous terms. The two steps Range-Kutta method is used for unsteady flow so as to obtain the second order accuracy in time and space.

Figure 3 is a comparison of experimental and computational shadowgraphs of the second example. The Reynolds number based on model diameter (12mm) for this test is near 10^5 . The test is performed at Mach number M_∞ of 15 and wall temperature T_w of 300K. Numerical simulation is based on full unsteady Navier-Stokes equations.

Table 1 shows in the first example the time cost comparison of one processor PC and the nine processors parallel system.

	distributing voxels	Resampling	Total cost
One processor	243 seconds	2018 seconds	2261 seconds
Nine processors	31 seconds	202 seconds	233 seconds

Table 1 Time cost comparison of one processor and nine processors system

1. Conclusion

By combining a spatial partitioning scheme with techniques which divided the flow field into regular regions, we have produced a parallel volume renderer for Computational Flow Imaging which employs inexpensive static load balancing to achieve high performance and reasonable efficiency with modest memory consumption. We believe that our algorithm has provide an effective way for rendering complex grids of Computational Flow Imaging on distributed-memory message-passing architectures. Detailed performance experiments with up to 9 processors lead us to believe that further improvements are possible.

We plan to conduct additional tests with larger datasets, different image sizes, more processors, and other architectures. With larger datasets, the number of ray segments generated may increase significantly, and we need to assess the impact of this additional communication load on overall performance. We also want to investigate the potential for finer-grained image partitionings and improved termination strategies to improve the parallel efficiency of our approach.

References

1. George Havener, "Computational Flow Imaging: Fundamentals and History," *AIAA-94-2615*
2. G. Havener, Leslie A. Yates, "Visualizing flow with CFI," *Aerospace America*, June 1994
3. Havener, A.G. and Obergefell, L.A. "Computational Interferometric Description of Nested Flow Fields, " *Optical Engineering*, Vol.24, N0.3, May/June 1985, pp. 441-445.
4. Tamura, Y., K. Fuji "Visualization for Computational Fluid Dynamics and the Comparison with Experiments, " *AIAA paper 90-3031*, August 1990.
5. Yates, L.A. "Images Constructed from Computed Flowfields, " *AIAA paper 92-4030*, AIAA 17th Aerospace Ground Testing Conference, Nashville, TN, July 1992
6. T.A.W.M. Lanen, E.M. Houtman and P.G. Bakker, "Comparison of interferometric measurements with 3-D Euler computations for circular cones in supersonic flow, " *AIAA-92-2691*.
7. Stacey G Rock, "CFI-Interferometry analysis of Hypervelocity Ballistic Flow Fields, " *AIAA-94-2617*
8. Wolfgang Merzkirch. "Flow Visualization, " *Academic Press*, 1974.
9. T.T.Elvens, "A Survey of Algorithms for Volume Visualization, " *Computer Graphics*, Vol.26, No.3, Aug. 1992, pp.194-201.
10. M. Snir, S. W. Otto, S. Huss-Lederman, D. W. Walker, and J. Dongarra. "MPI: The Complete Reference, " MIT Press, 1995.